http://dx.doi.org/10.5012/bkcs.2012.33.6.1890

Molecular Imaging of Arthritis in the Angiogenic Vasculature Using A ^{123}I-Vascular Endothelial Growth Factor Receptor Antibody

Sung-Min Kim,[†,a] Naeun Choi,[†,a] Youngkyu Song,[†,‡] Gyunggoo Cho,[†] Jeongkyu Bang,[†] Sang Mi Kim,[‡] Sang Hoon Lee,[‡,*] and Eun Kyoung Ryu[†,*]

[†]*Division of Magnetic Resonance Research, Korea Basic Science Institute, Chungbuk 363-883, Korea. [*]E-mail: ekryu@kbsi.re.kr*
[‡]*Department of Radiology and Research Institute of Radiology, University of Ulsan College of Medicine, Asan Medical Center, Seoul 138-735, Korea. [*]E-mail: shlee@amc.seoul.kr*
Received January 26, 2012, Accepted March 5, 2012

Vascular endothelial growth factor (VEGF) and its receptor (VEGFR) have been implicated in the pathogenesis of rheumatoid arthritis, which is angiogenesis dependent. Antibody-based molecular imaging improves targeting, and antibody radiolabeling is useful for monitoring biological events *in vivo via* PET or SPECT. We investigated the potential of molecular imaging to diagnose arthritis with VEGFR-2 *in vivo*. The ^{123}I-VEGFR-2 antibody was prepared by the iodogen tube method. The radioligand was injected into arthritic mice, and micro SPECT/CT was performed. The arthritic mice were examined by 4.7-T MRI and immunohistochemistry. The ^{123}I-VEGFR-2 antibody showed high uptake in the arthritic region at 1 h postinjection on SPECT/CT but no uptake in the control animals after radioligand injection. In MR images, the arthritic tissue of the mice was correlated with regions labeled by the ^{123}I-VEGFR-2 antibody. Immunohistochemical localization showed markedly increased expression of VEGFR-2 in the endothelial cells, fibroblasts, and macrophages of the arthritic mice.

Key Words : ^{123}I-VEGFR-2 antibody, VEGFR-2, Arthritis, Micro SPECT/CT

Introduction

Angiogenesis is a complex process through which new blood vessels grow from pre-existing vasculature.[1] Vascular endothelial growth factor (VEGF) and its receptor (VEGFR) act as essential factors for endothelial cell differentiation, proliferation, and migration in physiological and pathological angiogenesis, and they are strongly expressed in vascular endothelial cells.[2-5] VEGF and VEGFR are reported to be up-regulated in various diseases and play a significant role in tumor angiogenesis and inflammation.[6-9] VEGF- and VEGFR-based imaging agents have been used to improve the diagnosis and to selectively target the angiogenic vasculature.[10-12]

VEGF and VEGFR have been particularly implicated in the pathogenesis of rheumatoid arthritis (RA), which is considered to an angiogenesis-dependent disease. RA is characterized by the proliferation of cells of the synovial lining, neovascularization, infiltration of inflammatory cells, and synovial hyperplasia,[13,14] as well as increased microvessel density. The expression of VEGF-A, placenta growth factor (PIGF), and 3 VEGF tyrosine kinase receptors (VEGFR-1/Flt-1, VEGFR-2/KDR/Flk-1, and VEGFR-3) has been implicated in synovial angiogenesis in RA.[15] In RA, changes in the synovial tissue, cartilage, bone, and paraarticular soft-tissue components can be detected by contrast-enhanced MRI and high-resolution ultrasonography, which are more sensitive than other imaging modalities.[16,17] However, these methods cannot yield functional and metabolic information about RA.

Positron emission tomography (PET) and single-photon emission tomography (SPECT) are commonly used diagnostic modalities that are sensitive and widely used to study biological processes at the molecular level. The development of PET and SPECT probes is important for the early diagnosis of diseases. Many potential PET imaging agents for disease detection have been synthesized and evaluated. In particular, ^{18}F-FDG has been used as a metabolic tracer for the diagnosis of various tumors in human clinical trials and in animal studies. In addition, ^{18}F-FDG has been used for the diagnosis of arthritis in human patients because it is taken up by inflammatory lesions.[18,19] However, it is still difficult to apply ^{18}F-FDG for the evaluation of RA, which has a highly variable course that is difficult to predict.[20] Therefore, the development of sensitive and specific radioligands to detect early signs of RA is necessary.

Antibodies are commonly used in molecular imaging to improve targeting. Radiolabeled antibodies permit the monitoring of biological events in living subjects using PET. Therefore, in this study, we investigated the potential of molecular imaging to diagnose arthritis with a specific antibody, VEGFR-2, *in vivo*.

Experimental

Mouse anti-VEGFR-2/KDR/Flk-1(VEGFR-2) antibodies were purchased from R&D Systems Inc. (Minneapolis, MN, USA). Rabbit anti-VEGF antibodies were purchased from

[a]These authors contributed equally to this work.

Cell Signaling Technology Inc. (Danvers, MA, USA), and rat anti-CD31 and Cy3-conjugated anti-rat IgG antibodies were purchased from BD Biosciences (Franklin Lakes, New Jersey, USA). Biotin-conjugated secondary antibodies were purchased from Santa Cruz Biotechnology Inc. (Santa Cruz, CA, USA). PD-10 columns were purchased from Amersham Biosciences (Piscataway, NJ, USA), and other chemicals were purchased from Sigma-Aldrich (St. Louis, MO, USA). The radioactivity was measured using a dose calibrator (Biodex Medical Systems, Shirley, NY, USA). Micro SPECT/CT images were acquired using an Inveon micro SPECT/CT scanner (Siemens Medical Solutions, Malvern, PA, USA) and analyzed using the Inveon Research Workplace software (IRW, Siemens Medical Solutions, USA). All animal experiments were performed according to the guidelines issued by the Institute Animal Care Committee of the Korea Basic Science institute, which are in accord with NIH guidelines.

Synthesis of the ^{123}I-VEGFR-2 Antibody. The VEGFR-2 antibody (50 μg) was dissolved in 500 μL of 0.1 M sodium phosphate buffer (pH 7.4), and Na ^{123}I (37 MBq) solution was added. The mixture was stirred for 1 h at room temperature with constant shaking (400 rpm) using a Thermomixer (Eppendorf, Hamburg, Germany) and was purified using a PD-10 column and 0.1 M phosphate-buffered saline (PBS, pH 7.4).

Animal Model. Male DBA/1J mice (age 9-10 weeks, weight 20-25 g) were used for the CIA model. In the CIA model, the mice were injected subcutaneously into the tail with 100 μg of bovine type II collagen (5 mg/mL; Chondrex, Redmond, WA) emulsified in an equal volume of Freund's complete adjuvant, which was followed 3 weeks later by a booster injection of 100 μg of bovine type II collagen emulsified in Freund's incomplete adjuvant. The mice developed RA 1 week after the second injection. Two weeks after the second injection, imaging studies were performed.

Micro SPECT/CT and 4.7 T MR Imaging. The ^{123}I-VEGFR-2 antibody (5.12 ± 1.06 MBq/200 μL) was injected intravenously in control (n = 3) or arthritic mice (n = 3) through the tail vein. Micro SPECT images were acquired for 10 min and 40 min using micro CT and SPECT at 1, 4, and 20 h after injection. The images were registered using IRW software to obtain SPECT and CT fusion images.

The animals were examined using a 4.7-Tesla MR imaging system (BrukerBioSpec, Germany) equipped with a maximum gradient strength of 400 mT/m (horizontal bore size and diameter of 400 and 120 mm, respectively). Radio frequency transmission and reception were performed with a quadrature volume coil (35 mm diameter, Bruker). During MR scanning, the animals were anesthetized by inhalation of 1.0-1.5% isoflurane in a mixture of N_2O and O_2 (7:3) through a mask.

For each animal, T2-weighted images were acquired to confirm the increased water content in mice with pathologic conditions such as bone marrow edema and synovitis. The imaging parameters were as follows: TR, 3,200 ms; TE, 80 ms; slice thickness, 1 mm; field of view (FOV), 2.5 × 2.5 cm^2; matrix size, 256 × 256; and average number of samples, 4.

Histological Study of Arthritic Lesions. Frozen sections were used for histological analysis. The mouse knee tissues were embedded in OCT compound and sliced into 5-μm sections on a cryostat (Leica 1850, Leica Micro systems, Wetzlar, Germany). The sections were fixed with acetone at –20 °C for 20 min. Hematoxylin and eosin (H&E) staining was performed according to a conventional staining protocol. The sections were stained with hematoxylin for 5 min, rinsed under running tap water, and then stained with eosin for 2 min. The stained sections were dehydrated with 70%, 90%, and 100% ethanol and then imaged under a microscope (OLYMPUS IX81, Olympus Inc., Japan). The images were processed using image analysis software (Metamorph, Molecular Devices Inc., USA).

Immunostaining. Immunohistochemical analysis was peformed using the streptavidin-biotin method. In brief, sections were incubated for 5 min in PBS buffer containing 0.3% H_2O_2 and washed 3 times in PBS for 5 min. They were then incubated with 5% BSA at room temperature for 30 min and with the primary antibodies (rabbit anti-VEGF, rabbit anti-VEGFR-2, diluted 1:100) at 4 °C for 16-18 h. The sections were then washed 3 times in PBS for 5 min, incubated with secondary antibodies (biotin-conjugated anti-rabbit, diluted 1:200) at room temperature for 3 h, washed with PBS, and incubated with ABC reagent (Vector Laboratories, USA). The sections were visualized by staining with 3,3-diaminobendizine and 0.03% H_2O_2 followed by counter staining with hematoxylin. The images were processed using image analysis software (Metamorph). The colocalization of VEGFR-2 and CD31 was evaluated using immunofluorescence. The sections were incubated for 5 min in PBS buffer containing 0.3% H_2O_2 and washed 3 times in PBS for 5 min, followed by incubation in 5% BSA at room temperature for 30 min. They were then incubated with the primary antibodies (rabbit anti-VEGFR-2, rat anti-CD31, diluted 1:100) at 4 °C for 16-18 h. The sections were then washed 3 times in PBS for 5 min and incubated with the secondary antibodies (FITC-conjugated anti-rabbit IgG and Cy3-conjugated anti-rat IgG, diluted 1:200) at room temperature for 3 h. After incubation, the sections were washed 3 times in PBS for 5 min and then imaged using a fluorescence microscope (Olympus IX81, Olympus Inc., Japan). The images were processed using image analysis software (Molecular Devices LLC, Sunnyvale, CA, USA).

Results and Discussion

The diagnosis of arthritis remains difficult, and no effective radioligand is available for detecting arthritis using PET. In this study, a VEGFR-2 antibody was labeled with ^{123}I for SPECT imaging of VEGFR-2 expression (Fig. 1) in arthritic mice. Thus, we studied the feasibility of noninvasive imaging for arthritic patients by using a novel radioligand for SPECT.

The ^{123}I-VEGFR-2 antibody was prepared using a general electrophilic radioiodination method with an iodogen tube, which is an easy radiolabeling procedure for proteins. The

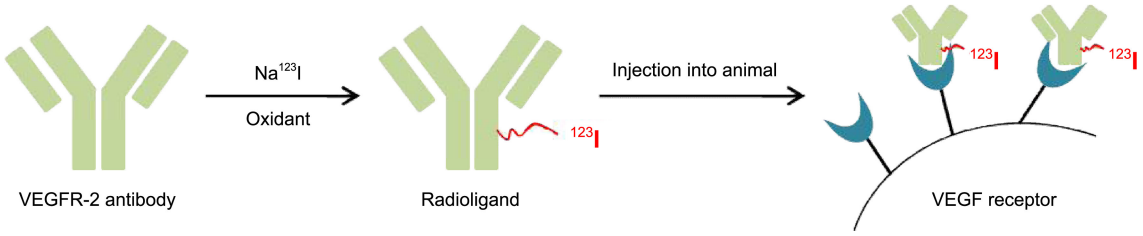

Figure 1. Tracing of VEGFR with the ^{123}I-VEGFR-2 antibody.

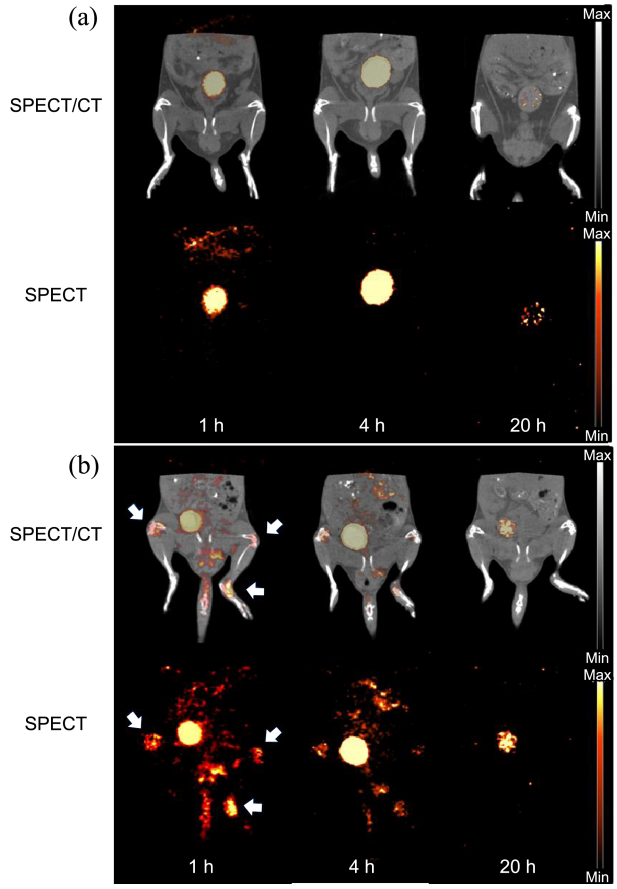

Figure 2. Micro SPECT/CT and SPECT images. Coronal images of the ^{123}I-VEGFR-2 antibody in normal (a) and arthritic mice (b) at 1, 4, and 20 h after injection *via* the tail vein. Arrows indicate radioligand uptake positions.

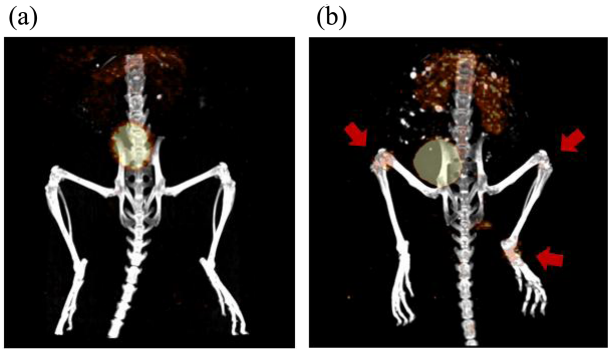

Figure 3. Micro SPECT/CT 3D images. Coronal images of the radiolabeled VEGFR-2 antibody in normal (a) and arthritic mice (b) at 1 h after injection. Arrows indicate radioligand uptake positions.

mixture was purified by exclusion chromatography (PD-10 column). The radiochemical yield was 20-25% with decay corrected, and the total synthesis required 70 min.

Micro SPECT/CT imaging studies were performed in wild-type and arthritic mice (Fig. 2). Static images (40 min) were obtained at 1, 4, and 20 h after the injection of the ^{123}I-VEGFR-2 antibody *via* the tail vein. High levels of radioactivity were detected in the bladder from 1 h postinjection, which indicates rapid excretion of the antibody. The arthritic knees and ankles showed a high uptake of the antibody from 1 h postinjection, and the levels decreased at 4 and 20 h. However, no uptake was observed in the knees and ankles of wild-type mice. No significant differences in the radioactivity of other organs were observed between the control and arthritic mice. The 3D SPECT-CT fusion image clearly

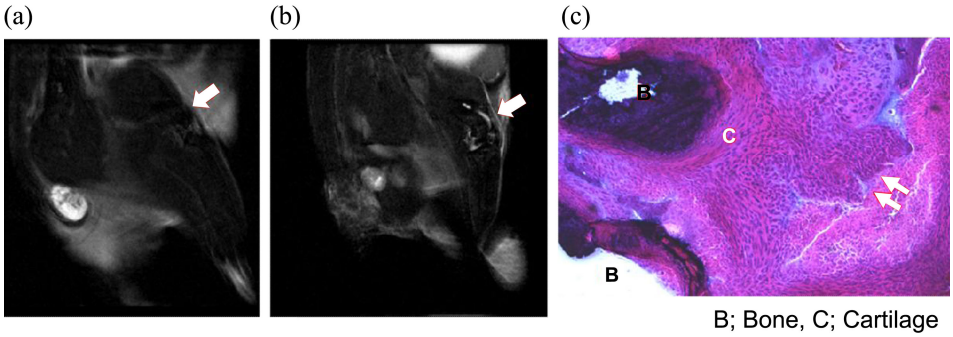

Figure 4. MR images of a normal mouse (a) andan arthritic mouse (b). Arrows indicate the knees of the mice. Joint effusion and suspicious synovial proliferation are present in the arthritic mouse. (c) Histological study of knee lesions in arthritic mice. Sections of knee tissue from wild-type and arthritic mice were stained with hematoxylin and eosin (H&E). H&E staining showed the disruption of articular cartilage, pannus formation, and infiltration into the cartilage in the arthritic knees (B: bone, C: cartilage; magnification, × 100).

showed the uptake of the ^{123}I-VEGFR-2 antibody in the arthritic region (Fig. 3), which indicates selective binding of the radioligand.

In the MR images, joint effusion and synovial thickening were seen in the knee joints of the arthritic mice (Fig. 4(b)). No joint effusion or synovial enhancement was seen in the knee joints of control mice (Fig. 4(a)). Erosion of the joint cartilage was not clearly seen, but bone marrow edema was observed at the distal femur and proximal tibia in the arthritic mice.

For histological evaluation of the arthritic lesions in the arthritic mice, we stained sections of the knee tissue from the arthritic mice with H&E (Fig. 4(c)). In the arthritic mice, the knee tissues showed marked infiltration of inflammatory cells into the joint space, hyperplasia of the synovium, invasive pannus formation, and bone and cartilage destruction. In addition, H&E staining showed chondrocyte disruption, granuloma formation, and the presence of infiltrating leukocytes in the arthritic mice.

Immunohistochemistry was used to localize VEGF and VEGFR-2 in the wild-type and arthritic mice. We found a marked increase in the expression of VEGF in endothelial cells, fibroblasts, and macrophages in the arthritic mice (Fig. 5). The expression of VEGFR-2 was significantly enhanced in the endothelial cells and fibroblasts of arthritic mice (Fig. 5). In addition, the angiogenesis marker CD31 was up-regulated in the arthritic mice. Alterations in the expression of VEGFR-2 occurred concurrently with alterations in the expression of CD31 (Fig. 6). Control immunostaining with normal mouse serum was completely negative in all animals.

^{123}I is useful for SPECT because it has a half-life of 6 hours and is easily radiolabeled with antibodies. Moreover, it can be modified to a positron-emitting isotope, such as ^{124}I, for PET imaging. Thus, the ^{123}I-VEGFR-2 antibody

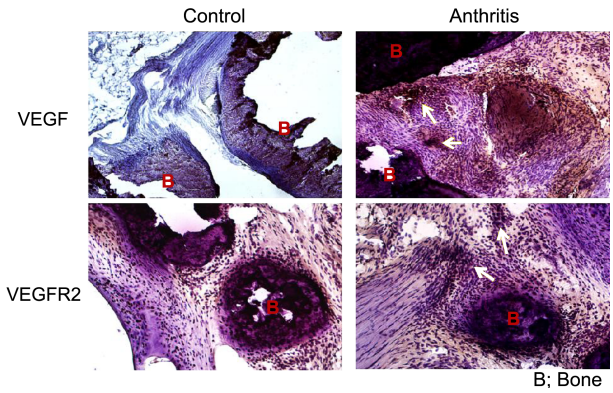

Figure 5. Expression of VEGF and VEGFR-2 in wild-type and arthritic mice. Expression of VEGF and VEGFR-2 in wild-type and arthritic mice; VEGF- or VEGFR-2-positive synoviocytes, endothelial blood cells, and synovial fibroblasts (arrow) (magnification, × 200).

showed specific binding to the wrist joint and knee; this finding was in agreement with the findings in MR images. SPECT is more sensitive than MRI because it can detect functional changes in molecules. VEGFR-2 is highly expressed in RA and can thus be used as a marker for early diagnosis. In our mouse model of arthritis, the SPECT images showed increased expression of VEGF and VEGFR-2, which agreed with the data obtained from immunohistochemistry and MRI.

Conclusion

The *in vivo* targeting and specific binding of the ^{123}I-VEGFR-2 antibody was assessed in arthritic mice by using SPECT imaging, and VEGFR-2-specific radioligand uptake was observed. Thus, the radiolabeled VEGFR-2 antibody

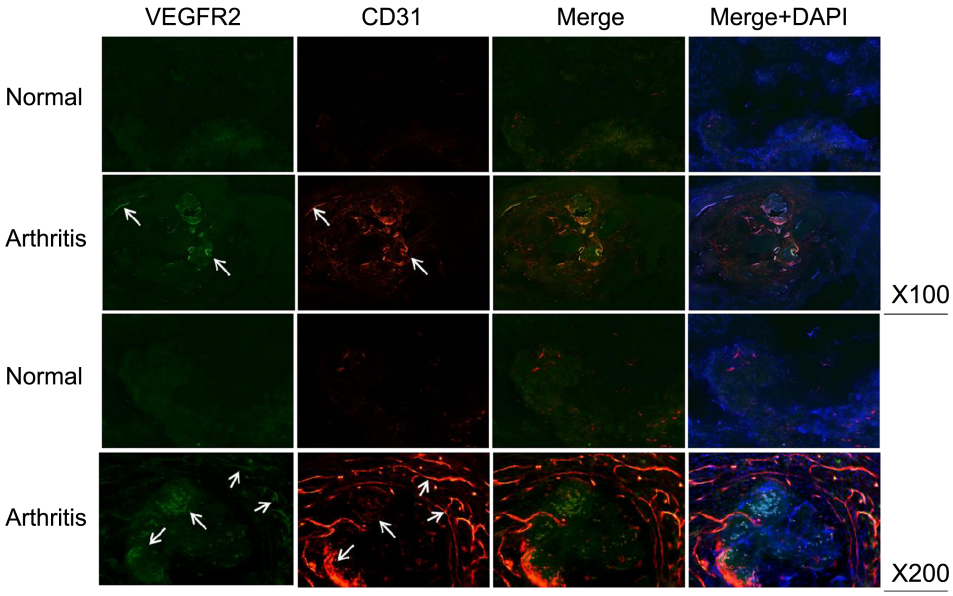

Figure 6. Immunofluorescence staining for VEGFR-2 and CD31 in arthritic mice. CD31 is expressed on the vascular endothelium. Immunofluorescence images of mouse CD31 (red), mouse VEGFR-2 (green), and merged VEGFR-2 and CD31 staining (yellow) demonstrate the expression of VEGFR-2 on endothelial cells and endothelial blood cells (original magnification, × 100 and × 200).

could be a potential radioligand for detecting arthritis using SPECT.

Acknowledgments. This research was supported in part by a grant from Korea Basic Science Institute (F32605) and a National Research Foundation of Korea (NRF) grant funded by the Korean government (MEST) (No. 2011-0027525).

References

1. Walsh, D. A. *Rheumatology (Oxford)* **1999**, *38*, 103.
2. Mustonen, T.; Alitalo, K. *J. Cell Biol*. **1995**, *129*, 895.
3. Ferrara, N.; Davis-Smyth, T. *Endocr. Rev*. **1997**, *18*, 4.
4. Jakeman, L. B.; Winer, J.; Bennett, G. L.; Altar, C.A.; Ferrara, N. *J. Clin. Invest*. **1992**, *89*, 244.
5. Yamane, A.; Seetharam, L.; Yamaguchi, S.; Gotoh, N.; Takahashi, T.; Neufeld, G.; Shibuya, M. *Oncogene* **1994**, *9*, 2683.
6. Shibuya, M. *Cell Struct. Funct*. **2001**, *26*, 25.
7. Luo, J. C.; Toyoda, M.; Shibuya, M. *Cancer Res*. **1998**, *58*, 2594.
8. Carmeliet, P.; Moons, L.; Luttun, A.; Vincenti, V.; Compernolle, V.; De Mol, M.; Wu, Y.; Bono, F.; Devy, L.; Beck, H.; Scholz, D.; Acker, T.; DiPalma, T.; Dewerchin, M.; Noel, A.; Stalmans, I.; Barra, A.; Blacher, S.; Vandendriessche, T.; Ponten, A.; Eriksson, U.; Plate, K. H.; Foidart, J. M.; Schaper, W.; Charnock-Jones, D. S.; Hicklin, D. J.; Herbert, J. M.; Collen, D.; Persico, M. G. *Nat. Med*. **2001**, *7*, 575.
9. Ferrara, N.; Gerber, H. P.; LeCouter, J. *Nat. Med*. **2003**, *9*, 669.
10. Li, S.; Peck-Radosavljevic, M.; Kienast, O.; Preitfellner, J.; Havlik, E.; Schima, W.; Traub-Weidinger, T.; Graf, S.; Beheshti, M.; Schmid, M.; Angelberger, P.; Dudczak, R. *Q. J. Nucl. Med. Mol. Imaging* **2004**, *48*, 198.
11. Lu, E.; Wagner, W. R.; Schellenberger, U.; Abraham, J. A.; Klibanov, A. L.; Woulfe, S. R.; Csikari, M. M.; Fischer, D.; Schreiner, G. F.; Brandenburger, G. H.;. Villanueva, F. S. *Circulation* **2003**, *108*, 97.
12. Backer, M. V.; Levashova, Z.; Patel, V.; Jehning, B. T.; Claffey, K.; Blankenberg, F. G.; Backer, J. M. *Nat. Med*. **2007**, *13*, 504.
13. Murakami, M.; Iwai, S.; Hiratsuka, S.; Yamauchi, M.; Nakamura, K.; Iwakura, Y.; Shibuya, M. *Blood*. **2006**, *108*, 1849.
14. Kim, W. U.; Kang, S. S.; Yoo, S. A.; Hong, K. H.; Bae, D. G.; Lee, M. S.; Hong, S. W.; Chae, C. B.; Cho, C. S. *J. Immunol*. **2006**, *177*, 5727.
15. Hoeben, A.; Landuyt, B.; Highley, M. S.; Wildiers, H.; Van Oosterom, A. T.; De Bruijn, E. A. *Pharmacol. Rev*. **2004**, *56*, 549.
16. Donohoe, K. J.; Henkin, R. E.; Royal, H. D.; Brown, M. L.; Collier, B. D.; O'Mara, R. E.; Carretta, R. F. *J. Nucl. Med*. **1996**, 37, 1903.
17. Backhaus, M.; Burmester, G. R.; Sandrock, D.; Loreck, D.; Hess, D.; Scholz, A.; Blind, S.; Hamm, B.; Bollow, M. *Ann. Rheum. Dis*. **2002**, *61*, 895.
18. Palmer, W. E.; Rosenthal, D. I.; Schoenberg, O. I.; Fischman, A. J.; Simon, L. S.; Rubin, R. H.; Polisson, R. P. *Radiology* **1995**, *196*, 647.
19. Beckers, C.; Ribbens, C.; Andre, B.; Marcelis, S.; Kaye, O.; Mathy, L.; Kaiser, M. J.; Hustinx, R.; Foidart, J.; Malaise, M. G. *J. Nucl. Med*. **2004**, *45*, 956.
20. Brenner, W. *J. Nucl. Med*. **2004**, *45*, 927.